PCCP

Accepted Manuscript

ROYAL SOCIETY OF CHEMISTRY

www.rsc.org/pccp

O^- from Amorphous and Crystalline CO_2 Ices

Daly Davis, Sramana Kundu, Vaibhav S. Prabhudesai and E. Krishnakumar* [a]

O^- desorbed from amorphous and crystalline films of CO_2 at 18 K under low energy electron impact is studied using time of flight mass spectrometry. The nature of the CO_2 film is characterized using Fourier transform Infrared spectrometry as a function of film thickness. It is found that the desorption rate from amorphous films are considerably larger than that from crystalline films. The desorption signal from the 4 eV resonance is found to be the dominant one as compared to that from the higher energy resonances, notably the one at 8 eV observed in the gas phase. This is explained in terms of the large enhancement in the dissociative electron attachment cross section for the 4 eV resonance in the condensed phase reported earlier using the charge trapping method.

1 Introduction

Dissociative Electron Attachment (DEA) is one of the important processes in low energy electron (LEE) collisions on molecules. Recent gas phase experiments show that DEA allows control of chemical reactions through selective bond cleavage [1,2]. Selective bond breaking is possible by tuning the electron energy to the respective resonant energy. In addition, recent theoretical investigations have shown the role of LEE as catalysts in bond breaking through resonant attachment [3,4]. Low-energy electron irradiation experiments in pure ices condensed at cryogenic temperatures have attracted considerable interest within the last few years as a model that simulates the electron induced reactions in the interstellar [5] and biological [6] conditions.

Carbon dioxide is one of the fundamental and most studied polyatomic molecular constituents of the planetary atmosphere [7]. It has been investigated by almost all the spectroscopic techniques available. There have been reports which describe the CO_2 chemistry in the interstellar medium [8]. Because of its simplicity CO_2 is one of the best candidates for the development of theoretical modeling and calculations in molecular physics. Yet one can find several unexplored areas in CO_2 induced chemistry. For example, a very recent report showed that CO_2 films crystallize as they grow in thickness. This study also indicated the absence of amorphous CO_2 ice in space [9].

CO_2 molecule has a negative electron affinity of 0.6 eV and the electron attachment leads to a bent state of CO_2^- [10]. LEE scattering experiments show mainly two resonance states for gas phase CO_2, a shape resonance ($^2\Pi_u$) at 4 eV [11] and a Feshbach resonance ($^2\Pi_g$) at 8 eV [12]. Cluster formation of CO_2 induces changes in electron binding, and hence, alters energy and properties of resonances. For example, while in single CO_2 only O^- is generated via DEA, LEE attachment to clusters leads to the homologous series $(CO_2)_n^-$ and $(CO_2)_nO^-$ [13]. Electron-Attachment studies on CO_2 clusters also showed that cluster to bulk transition occurs at a critical size of 30 monomers of CO_2 [14].

Very few experiments have been reported on low energy electron collision on CO_2 ices, except for the work by Sanche and colleagues. Three different studies have been conducted by them on low energy electron collision on CO_2 films at low temperatures. In the first one they reported the electron stimulated desorption of O^- and metastable CO from physisorbed CO_2 [15]. They observed four peaks (at ∼4.1, 8.5, 11.2 and 15 eV) in the O^- yield as a function of electron energy. In another experiment using charge trapping method, they observed that the absolute cross sections for anion production from CO_2 deposited on multilayer Kr substrate is enhanced about 43 times in the condensed phase as compared to that in the gas phase for the 4 eV resonance [16]. The third experiment provided low energy electron scattering cross section for the production of CO within thin solid films of CO_2 condensed on an Ar multilayer substrate [17]. All these studies have been carried out on amorphous films of CO_2. In this report we present results on electron stimulated desorption of O^- from amorphous and partially crystalline films of CO_2. We base our studies on the recent observation that CO_2 films crystallize as they grow in thickness and that there are distinct infrared bands in the CO_2 spectrum that distinguish the amorphous state from the crystalline state [9]. We also use a Time of Flight (ToF) spectrometer for mass analysis which does not discriminate the ions for their kinetic energies. We find that the desorbed O^- signal is considerably smaller from crystalline films as compared to that from amorphous films and that the signal from the 4 eV resonance is much larger as compared to the ones at higher energies. These two observations may have important consequence in the context of modelling CO_2 based chemistry in the astrophysical situations considering that most of the CO_2 ice in space is crystalline in nature [9].

[a] *Tata Institute of Fundamental Research, Mumbai - 400005, India. Fax: +91-22 2280 4610; Tel: +91-22 2278 2502; ekkumar@tifr.res.in*

2 Experimental Method

The measurements are carried out in our new experimental set up designed for condensed phase studies. The assembly consists of an electron source, a cold substrate for sample deposition and a ToF Spectrometer, built in house, to detect the anions that are desorbed from the solid. They are enclosed in a hexagonal oil free ultra-high vacuum (UHV) chamber reaching base pressure of 2×10^{-10} Torr.

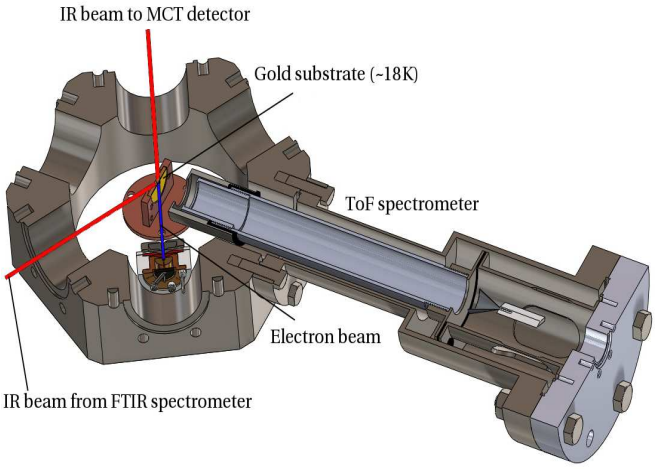

Fig. 1 A schematic view of the assembly with ToF mass spectrometer

The schematic of the experimental setup is shown in Fig. 1. The electron source is a compact home built three element gun of Pierce geometry. It is pulsed by cutting off the current using a reverse bias on the grid and overriding it with a positive pulse. The beam is collimated by a magnetic field produced by a pair of coils in Helmholtz geometry mounted outside the vacuum chamber. The electron beam is allowed to impinge on the substrate at 60^o with respect to the substrate normal. The energy resolution of the electron beam in this experiment is about 0.5 eV. The time averaged electron current, as measured at the target, is about 0.7 nA for collision energies ranging between 2 and 20 eV at a repetition rate of 50 kHz and a pulse width of 100 ns.

The molecules are deposited on the (1 0 0) plane of a crystalline gold substrate of diameter 20 mm mounted on a cold head ($\sim$18 K) connected to a closed cycle helium refrigerator. Temperature of the substrate is controlled by a Si-diode sensor and UHV heater looped to a temperature controller. Temperature calibration is carried out using the phase change of ammonia ice [18] film in an independent set of experiments in the same set up. This is found to be within 1 K and corrected accordingly. Thickness of the deposited film is measured by reflection absorption infrared (RAIR) spectroscopy using a Nicolet 6700 FTIR spectrometer. IR beam from the spectrometer probes the molecular film deposited on the side opposite to the one where electron irradiation is carried out. This is done at an angle of 60^o with respect to the substrate normal [Fig. 1]. All the background CO_2 and water from the IR beam path is purged out using dry nitrogen. The RAIR spectra are recorded for 72 scans at a resolution of 2 cm^{-1} using a liquid nitrogen cooled mercury cadmium telluride (MCT) detector kept at 120^o to the incoming IR beam. Fast Fourier transform is done by the computer programme. Background deposition method has been used to produce uniform films. Samples are deposited using a needle valve by flowing through a 0.25 inch diameter tube kept symmetrically about the substrate so that the deposition on both sides are the same. The gold substrate, the heater and the temperature sensor are mounted on a specially designed holder made of oxygen free high conductivity copper which is electrically isolated from the cold head by using a sapphire plate of 2 mm thickness.

The ToF spectrometer is mounted right in front of the gold substrate with its axis normal to the substrate. The entrance aperture to the ToF Spectrometer is kept at a distance of 13 mm from the gold substrate and grounded. Negative ions produced on the surface are pushed into the ToF spectrometer by a pulsed electric field. This ion extraction field is generated by applying a negative pulse of 1μs width to the gold substrate, with a delay of 100 ns after the electron pulse. The ToF spectrometer is of Wiley McLaren geometry [19] and the flight tube voltage is optimized for a given ion extraction field. For the best mass resolution and for 60 V on the gold substrate, a voltage of 160 V on the flight tube is found to give optimum performance. The ions are detected using a channel electron multiplier operated in the pulse counting mode. The signal from it, after due amplification, fed into the 'STOP' input of a multihit card which had a time resolution of 500 *p*s. The 'START' pulse for this card is generated after suitable delay from the master pulse generator that controls the pulse generators used for pulsing the electron beam and the ion extraction field. In the present experiment the electron energy is ramped from 0 to 20 V in 0.2 V steps and the mass spectra are stored as a function of electron energy. The ion yield curve for any ion of particular mass to charge ratio *(m/e)* could be generated by analysing the mass spectra. A specially built software is used for data recording, data analysis and for control of the programmable power supply, which defines the electron energy.

3 Results and Discussion

3.1 Oxygen

The overall performance of the experimental set up has been tested by carrying out measurements on a pure multilayer film

of O_2. Multilayers of oxygen (99.9998%) are deposited at 26 K. At this temperature oxygen solidifies as β crystalline form[20]. Signature of crystalline nature of the solid film can be observed as a peak centred at around 1600 cm^{-1} in the RAIR spectrum shown in Fig. 2. The noisy looking bands on either side of the peak are due to the P and R bands of water. Around 1600 cm^{-1} there are no water bands, which allows the observation of the rather weak band of O_2.

It has been reported that the well known peak at 6.5 eV observed in the DEA signal in gas phase O_2 manifests as a peak at around 8.1 eV in pure amorphous films of O_2[21]. We observed a O^- peak at around 9.4 eV (Fig. 3). It is not clear if the difference between the two measurements is due to the film being amorphous or crystalline. It is possible that the shift of ∼1.3 eV could mainly be due to charge trapping in the thick film of oxygen even though oxygen is in the crystalline phase[22]. Change of substrate from platinum to gold could also contribute a little to DEA by change in orientation of the molecules deposited. But the thickness of the oxygen film deposited is large enough to neglect the substrate effect.

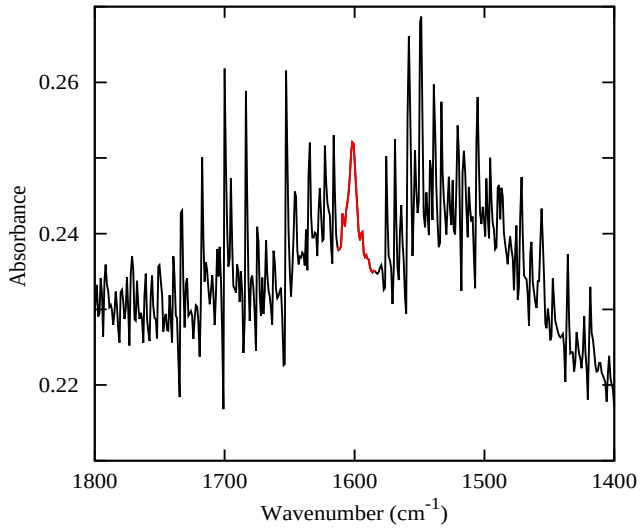

Fig. 2 RAIR spectrum of crystalline O_2 deposited at 26 K. The peak centred at around 1600 cm^{-1} (shown in red colour) is the signature of the β crystalline structure. The noisy looking bands on either side of the peak are due to the P and R bands of water.

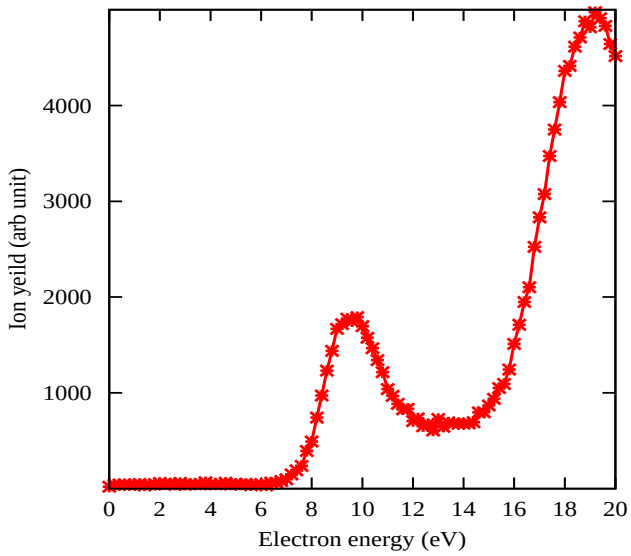

Fig. 3 Ion Yield curve for O^- from O_2. The peak at 9.4 eV is due to the DEA process. The signal at higher energies is dominated by the polar dissociation process.

3.2 Carbon dioxide

We deposited 99.995% pure CO_2 at various thickness at around 18 K. Thickness of the deposited films is calculated using column density, N,

$$N = \frac{cos\theta}{2} \frac{\int_{band} \tau_\nu \, d\nu}{A} \quad (1)$$

where τ_ν is the optical depth of the band, $d\nu$ is the wave number differential (in cm^{-1}), and A is the band strength (in cm $molecule^{-1}$). Factor of $\cos\theta/2$ accounts for the path length covered by IR beam due to reflection and the increase in pathlength due to the angle of incidence, θ, of the IR beam. Since, as described below, the ν_3 stretching band of $^{12}C{=}O$ of the dominant isotopomer of CO_2 shows broad distribution depending on the structural composition of the ice, we used the same band of $^{13}C{=}O$, which appears at 2283 cm^{-1} as a single peak, for monitoring the thickness. Band strength A for ν_3 $^{13}C{=}O$ is 7.8×10^{-17}, [23] and the isotopic concentration of ^{13}C is 1.07%. The ν_3 stretching band of $^{13}C{=}O$ at 2283 cm^{-1} at different thickness are shown in Fig. 4. The number of monolayers are calculated by assuming 1 x 10^{15} molecules per cm^2 for 1 monolayer of coverage.

We compared the thickness measurement using RAIR spectroscopy with a direct deposition method using an effusive source of known geometry in a separate set of experiments, similar to that described by Madey[24] and Sanche[25]. For this we mounted an aperture 1 mm thick and 1 mm in diameter concentrically in front of the substrate at a distance of 50 mm such that the normal to the surface passed through the aperture. A stainless steel container of 1 litre volume was connected to the aperture and CO_2 was filled in it at room temperature at a pressure of 1 Torr as measured by a capacitance manometer. A finite quantity of gas was leaked through the aperture when the substrate was cooled to 18 K and the pres-

sure drop in the container was noted. From the volume and the pressure drop, the total number of molecules effused into the vacuum chamber was calculated. Using the geometric factors, the number of molecules falling on unit area of the substrate was then calculated using the angular distribution of effusive beam as given by Clausing[26]. This was then converted into the the number of monolayers assuming unit sticking efficiency. The film thickness was also measured using RAIR spectroscopy simultaneously. We found that the gas dosage method gave about a factor of two larger thickness.

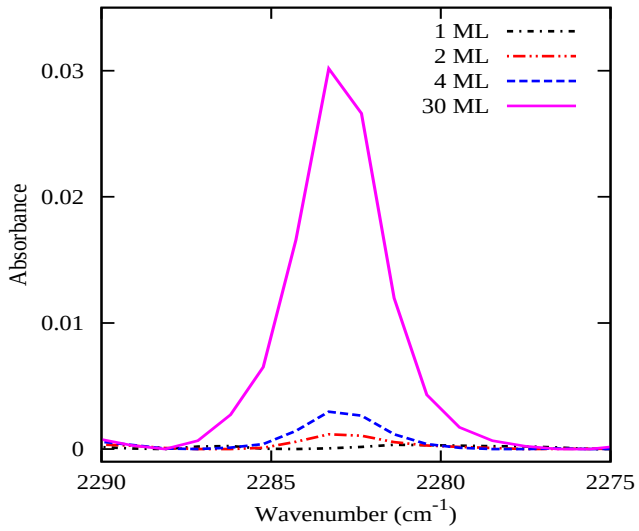

Fig. 4 The ν_3 stretching band of $^{13}C{=}O$ in $^{13}CO_2$ at 2283 cm^{-1} as a function of film thickness.

Fig. 5 shows the RAIR spectra of CO_2 deposition at different thickness. The spectrum at 30 ML thickness clearly shows two strong peaks at 2343 cm^{-1} and 2380 cm^{-1} and a shoulder at 2328 cm^{-1}. At lower thickness the spectra are dominated by the peak at 2380 cm^{-1} with small peaks at 2343 cm^{-1} and 2328 cm^{-1} respectively. For the 1 ML thick film, the 2380 cm^{-1} peak is slightly red shifted to 2378 cm^{-1}. A recent work on crystallization of CO_2 ice has shown that by thermal annealing complete crystallization of CO_2 from amorphous phase of the films occurs at 30 K[9]. This is characterized by disappearance of a peak at 2328 cm^{-1} and appearance of a peak at 2343 cm^{-1}. They also showed that the crystallization process is taking place in the sample films during its growth even at low temperatures (14 K). Using transmission IR spectroscopy at normal incidence they observed the presence of crystalline CO_2 as a peak appearing at 2343 cm^{-1}, for thickness larger than 20 ML. They assigned the IR band near 2328 cm^{-1} to the amorphous form of CO_2. In addition to the IR observations, Ingolfsson *et al*[14,27] showed that in CO_2

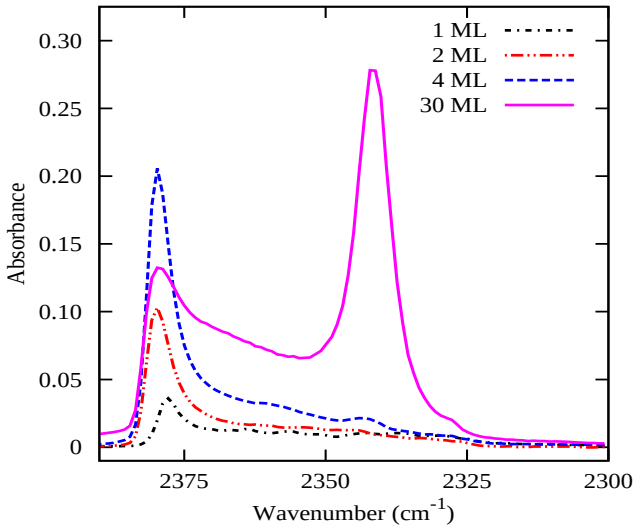

Fig. 5 IR spectra of CO_2 as a function of thickness.The spectrum at 30 ML thickness clearly shows two strong peaks at 2343 cm^{-1} and 2380 cm^{-1} and a shoulder at 2328 cm^{-1}. At lower thickness the spectra are dominated by the peak at 2380 cm^{-1} with small peaks at 2343 cm^{-1} and 2328 cm^{-1} respectively. For the 1 ML thick film, the 2380 cm^{-1} peak is slightly red shifted to 2378 cm^{-1}.

aggregates, cluster to bulk transition occurs above about 30 monomers of CO_2 and dominates for 55 monomers of CO_2, with face-centered cubic bulk packing. Also, it is well known that in IR spectroscopy of crystals, oblique angles give rise to Berreman effect, i.e., splitting of reflection and transmission frequencies into longitudinal optical (LO) and transverse optical (TO) modes[28]. TO modes are characterized by atomic displacements perpendicular to the wave vector, whereas, for LO vibrations the atomic displacement are parallel. The Berreman effect has been observed not only in crystals, but also in several amorphous materials like TiO_2,[29] silica glass etc[30]. It has also been shown that in RAIR spectra of thin films of CO and CO_2 on a metal surface like gold, only LO mode is observed, in oblique angles, even for films of thickness 8 nm[31,32]. The TO mode could not be observed at lower thickness, since in a metal the electric field close to the surface is normal to the surface[31]. In the present work, we see a peak due to amorphous CO_2 at 2328 cm^{-1}. The peak at around 2380 cm^{-1} is due to LO mode of amorphous and crystalline CO_2. This peak is shifting towards higher energy with increase in film thickness, which indicates the development of crystalline structure with film thickness[9]. At 4 ML thickness the crystalline peak at 2343 cm^{-1} starts showing up and at 30 ML thickness this band (2343 cm^{-1}) is the strongest. As mentioned earlier, the TO mode, which appears at 2343 cm^{-1}gets enhanced only at

larger thickness. This explains the larger intensity at 2343 cm^{-1} as compared to that at 2380 cm^{-1}. At small thickness the TO band (2343 cm^{-1}) is considerably smaller as compared to the LO band (2380 cm^{-1}) and has an intensity less than that of the amorphous CO_2 (2328 cm^{-1}) band. Table 1 gives the ratio of the intensities at 2343 cm^{-1} and 2328 cm^{-1} for films of various thickness. It can be seen that at 4 ML thickness the intensity of the TO band is comparatively larger indicating the presence of both amorphous and crystalline structure and at 30 ML it is dominated by the crystalline structure. Thus based on the IR spectrum we characterize the CO_2 films as amorphous, a mixture of amorphous and crystalline or dominantly crystalline. In short we are able to control the structure of the CO_2 film as amorphous or crystalline based on its thickness at temperatures lower than 30 K.

Table 1 Intensity of the 2343 cm^{-1} band to 2328 cm^{-1} band as a function of film thickness

Thickness (ML)	I (2343 cm^{-1})/I (2328 cm^{-1})
30	273.4
4	5.13
2	0.96
1	0.42

We measured the negative ions emitted from the CO_2 film under low energy electron impact using the ToF mass spectrometry. The spectra showed the presence of only O^- ions. This is in accordance with what has been reported [15]. Fig. 6 shows the yield of O^- ions from the CO_2 films at various thickness as a function of electron energy, integrated over 10 scans. The energy scan took around 16 minutes to complete. As shown in the Fig. 6, we observe one broad peak below 8 eV from all the four films. For the 30 ML and 4 ML films this peak is centred at 4 eV. It is blue shifted to 5.4 eV for 2 ML and 5.2 eV for 1 ML films, respectively. We note that the entire ion yield curve for the 2 ML film is more blue shifted. This may be due to slightly excess charge trapping of this film as compared to the 1 ML film and thereby causing a corresponding energy shift of the electrons. The other feature apart from the steadily increasing intensity beyond 16 eV is the peak centred about 11 eV that is seen clearly from the 1 ML film and as a broader structure from the 2 ML film. The peak seen at about 4 eV from the partly crystalline films (4 ML and 30 ML) and at slightly higher than 5 eV from the amorphous films (1 ML and 2 ML) could be attributed to the resonance seen at 4 eV in the gas phase DEA to CO_2. The peaks at 8.5 eV and 15 eV reported by Sanche and co-workers [15] are not clearly visible in our data. As the reported peaks at higher energies have width as high as 2 eV, the absence of these peaks as clear structures in our data may not be due to poorer electron energy resolution in our experiments. We believe that it is due to relatively larger charge trapping in our experiment. We note that Huels *et al.* [15] had found that the negative ions due to the 4 eV resonance start appearing only when the film is charged to about 0.8 eV. We too observe this phenomenon. The 4 eV feature is associated with a short lived $^2\Pi_u$ shape resonance which dissociates into O^- and CO fragments. The O^- produced in this process has very little kinetic energy to escape from the binding of the solid matrix. Only when sufficient negative charge has accumulated locally in the film (sufficient to produce the energy shift of the order of 0.8 eV), some of the DEA produced O^- fragments will get ejected into the vacuum [15]. They further observed that with charging, the peaks observed at higher energies reduce in intensity and become distorted. In the present experiment, the charge trapping is slightly larger as seen from the shift of the 4 eV resonance to a little over 5 eV for the case of the amorphous films. It is possible that with larger charge trapping, the higher energy resonances observed by Huels *et al.* are further reduced in intensity and lose the distinctive peak structure.

One of the important aspects of the present results is the dominance of the lowest resonance (~4 eV) and the overall reduction in the O^- signal as the structure of the film is changed from amorphous to crystalline. As mentioned above, the feature near 4 eV appears only after enough charging of the amorphous films [15]. In the amorphous form the intensity of the peak is almost same for films of thickness 2 ML and 1 ML. Also, in both cases, the 4 eV peak is blue shifted by a little more than 1

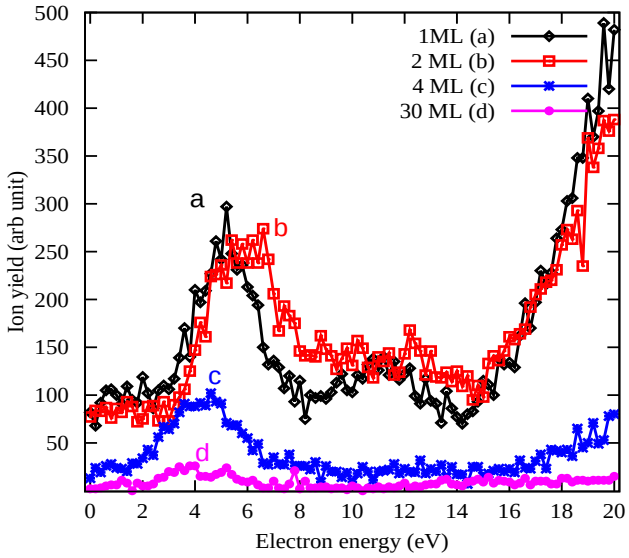

Fig. 6 Ion Yield curve for O^- from CO_2 as a function of film thickness. The changes in the ion yield curves in structure as well as in intensity as the film composition changes from amorphous to crystalline with increasing thickness may be noted. (a, b - amorphous CO_2 and c, d - partially crystalline CO_2)

eV. The energy shift to higher values confirms efficient charge trapping in amorphous films. In partially crystalline form the intensity of the 4 eV feature reduces considerably. It is found to be present but with further reduced intensity in the case of the 30 ML film where we observe maximum crystalline structure. As discussed earlier, the 4 eV peak is attributed to the resonance decaying into low energy O^- fragment which needs higher trapped charge for gaining sufficient energy to escape the surface. Amorphous form traps charge more efficiently due to their random orientation. Whereas in crystalline form charge can penetrate through the crystal lattice[22]. The influence of charge trapping on 4 eV feature is clear in Fig. 6. The reduction in intensity of the 4 eV peak with increased thickness and hence due to increased crystalline form of the target points to this effect. Besides, the resonance lifetime against autodetachment can vary due to crystalline nature of the target. The reduction of 4 eV peak may be due to this reduction in the survival probability of the resonance in the crystalline phase.

The broad structure seen between 8 and 16 eV in the case of thinner (1 ML and 2 ML) films appear to diminish considerably in intensity for the thicker (4 ML and 30 ML) films. As mentioned above, in this region Huels *et al.*[15] had observed three resonances. The reduction in intensity with increasing thickness of condensed CO_2 indicates the less efficient formation of the resonances in the crystalline phase as against the amorphous phase as well as lower survival probability of the resonance against auto detachment. The peak around 12 eV has been attributed to the cluster nature of CO_2 deposit[15]. Crystallinity reduces the cluster nature of the condensed phase and thus may explain the disappearance of 12 eV peak.

The O^- signal due to polar dissociation (for electron energy above 14 eV) from the CO_2 film is found to be reducing with increasing thickness. The O^- fragment from polar dissociation is generally known to be formed with low kinetic energy. Hence, its behaviour is also expected to be similar to the 4 eV resonance in the O^- channel. However, one important difference in the two channels is that for polar dissociation no resonance formation is needed; but efficient inelastic scattering of electrons within the target molecules is essential. The reduction in the polar dissociation signal with increasing film thickness and subsequent change to crystalline phase of the target may also indicate lower probability of such inelastic scattering.

The dominance of the 4 eV peak over higher energy ones in all the films, independent of their structure, needs to be explained. As discussed earlier, charge trapping method has been used to show that DEA cross section for the 4 eV resonance in condensed phase is much larger (43 times) than that in gas phase, while the the resonance at 8 eV, which has a cross section about three times that of the 4 eV resonance in gas phase, did not show any noticeable enhancement[16]. We also observe larger signal from the 4 eV resonance as compared to that at higher energies. However, the O^- desorption studies from condensed films indicated that the signal at 4 eV is smaller (as much as a factor of 10) than those at higher energies[15]. This may be due to the difference in detection techniques employed in the two measurements. The measurements by Huels *et al*[15] were done by detecting the negative ion signal using a quadrupole mass spectrometer mounted at an angle of 20^o to the normal to the substrate. Also, in those measurements no electric field has been used to extract the ions into the mass spectrometer. Hence, it is possible that in that experiment there might have been a large discrimination against very low energy ions. In our experiment we use a strong extraction field to force the ions into the ToF mass spectrometer. Moreover, this spectrometer has its axis normal to the substrate. Thus it does not have any discrimination with respect to the ion energy. For films of smaller thickness, which are amorphous, we find that O^- signal is about a factor of 2 larger as compared to that at higher energies. Since the O^- ions formed at 4 eV have considerably smaller kinetic energy as compared to those formed at 8 eV, the desorption of the ions into the vacuum at 4 eV is expected to be relatively smaller. This implies that the production of O^- at 4 eV should be higher than what is actually observed by us. Our observation of larger signal at 4 eV as compared to that at higher energies is consistent with the enhancement of the cross section observed for the 4 eV resonance using the charge trapping technique[16] and is a direct evidence of the enhancement of the cross section of the 4 eV resonance as compared to that at higher energies.

4 Summary and Conclusions

We have presented the desorption measurements of the O^- ions from amorphous and crystalline form of CO_2 using a newly built condensed phase experimental set up that incorporates a ToF mass spectrometer for negative ion detection. The amorphous or crystalline nature of the film is diagnosed using FTIR spectrometry. The desorption signal from the 4 eV resonance is found to be considerably larger than those from the higher energy resonances. Indirect measurements using the charge trapping technique had shown larger cross section for the production of O^- ions within amorphous films at the 4 eV resonance. The present measurements provide a direct measurement of the enhancement in the negative ion production from such films at the 4 eV resonance as compared to that at higher energies. We also find larger desorption of O^- from the amorphous film as compared to that from crystalline film. The dominance of the 4 eV resonance in the condensed phase and a significantly larger fraction of O^- produced at this energy is desorbed into the vacuum could have implications in the electron induced chemistry of CO_2 ice. Also, since most

of the CO_2 ice in space is crystalline in nature, the lower rate of production of O^- from crystalline films as compared to that from amorphous films could have considerable impact on the modelling of CO_2 based chemistry in space.

Acknowledgement

We acknowledge the support of Satej Tare, Yogesh Upalekar, Atiqur Rahman and Dr. Bhala Sivaraman for their help in building the experiment. We also thank Dr. T. S. Ananthakrishnan (BARC) and Prof. S. V. K. Kumar for the data acquisition software.

References

1 V. S. Prabhudesai, A. H. Kelkar, D. Nandi and E. Krishnakumar, *Phys. Rev. Lett.*, 2005, **95**, 143202–1–4.
2 S. Ptasińska, S. Denifl, V. Grill, T. D. Märk, E. Illenberger and P. Scheier, *Phys. Rev. Lett.*, 2005, **95**, 093201–1–4.
3 D. Davis, V. P. Vysotskiy, Y. Sajeev and L. S. Cederbaum, *Angew. Chem. Int. Ed.*, 2011, **50**, 4119–4122.
4 D. Davis, V. P. Vysotskiy, Y. Sajeev and L. S. Cederbaum, *Angew. Chem. Int. Ed.*, 2012, **51**, 8003–8007.
5 M. T. Sieger, W. C. Simpson and T. M. Orlando, *Nature*, 1998, **394**, 554–556.
6 B. Boudaffan, M. A. H. Pierre Cloutier, Darel Hunting and L. Sanche, *Science*, 2000, **287**, 1658–1660.
7 D. P. Cruikshank, A. W. Meyer, R. H. Brown, R. N. Clark, R. Jaumann, K. Stephan, C. A. Hibbitts, S. A. Sandford, R. M. E. Mastrapa, G. Filacchione, C. M. Dalle Ore, P. D. Nicholson, B. J. Buratti, T. B. McCord, R. M. Nelson, J. B. Dalton, K. H. Baines and D. L. Matson, *Icarus*, 2010, **206**, 561–572.
8 L. J. Sandford, S. A.; Allamandola, *Astrophys. J., Part 1*, 1990, **355**, 357–372.
9 R. M. Escribano, G. M. Muoz Caro, G. A. Cruz-Diaz, Y. Rodrguez-Lazcano and B. Mat, *Proc. Natl. Acad. Sci.*, 2013, **110**, 12899–12904.
10 R. N. Compton, P. W. Reinhardt and C. D. Cooper, *The Journal of Chemical Physics*, 1975, **63**, 3821–3827.
11 M. J. W. Boness and G. J. Schulz, *Phys. Rev. A*, 1974, **9**, 1969–1979.
12 C. R. Claydon, G. A. Segal and H. S. Taylor, *The Journal of Chemical Physics*, 1970, **52**, 3387–3398.
13 S. Denifl, V. Vizcaino, T. D. Mark, E. Illenberger and P. Scheier, *Phys. Chem. Chem. Phys.*, 2010, **12**, 5219–5224.
14 O. Ingolfsson and A. M. Wodtke, *The Journal of Chemical Physics*, 2002, **117**, 3721–3732.
15 M. A. Huels, L. Parenteau, P. Cloutier and L. Sanche, *J. Chem. Phys.*, 1995, **103**, 6775–6782.
16 M. A. Huels, A. D. Bass, P. Ayotte and L. Sanche, *Chem. Phys. Lett.*, 1995, **245**, 387 – 392.
17 M. C. Deschamps, M. Michaud and L. Sanche, *J. Chem. Phys.*, 2004, **121**, 4284–4291.
18 W. Zheng and R. I. Kaiser, *Chem. Phys. Lett.*, 2007, **440**, 229–234.
19 W. C. Wiley and I. H. McLaren, *Rev. Sci. Instrum.*, 1955, **26**, 1150–1157.
20 B. R. Cairns and G. C. Pimentel, *J. Chem. Phys.*, 1965, **43**, 3432–3438.
21 M. A. Huels, L. Parenteau1 and L. Sanche1, *J. Chem. Phys*, 1994, **100**, 3940–3956.
22 R. Balog, P. Cicman, D. Field, L. Feketeova, K. Hoydalsvik, N. C. Jones, T. A. Field and J.-P. Ziesel, *J.Phys. Chem. A*, 2011, **115**, 6820–6824.
23 P. A. Gerakines, W. A. Schutte, J. M. Greenberg and E. F. van Dishoeck, *Astron. Astrophys*, 1995, **296**, 810–818.
24 T. E. Madey, *Surface Science*, 1972, **33**, 355 – 376.
25 L. Sanche, *The Journal of Chemical Physics*, 1979, **71**, 4860–4882.
26 P. Clausing, *Zeitschrift fr Physik*, 1930, **66**, 471–476.
27 O. Ingolfsson and A. M. Wodtke, *Chem. Phys. Lett.*, 2002, **360**, 415 – 421.
28 D. W. Berreman, *Phys. Rev.*, 1963, **130**, 2193–2198.
29 B. C. Trasferetti, C. U. Davanzo, R. A. Zoppi, N. C. da Cruz and M. A. B. de Moraes, *Phys. Rev. B*, 2001, **64**, 125404.
30 R. M. Almeida, *Phys. Rev. B*, 1992, **45**, 161–170.
31 M. Elisabetta Palumbo, G. A. Baratta, M. P. Collings and M. R. S. McCoustra, *Phys. Chem. Chem. Phys.*, 2006, **8**, 279–284.
32 J. L. Edridge, K. Freimann, D. J. Burke and W. A. Brown, *Phil. Trans. R. Soc. A*, 2013, **371**, 20110578.